HHS Public Access

Author manuscript

Neuropharmacology. Author manuscript; available in PMC 2016 October 01.

Published in final edited form as:

Neuropharmacology. 2015 October ; 97: 464–475. doi:10.1016/j.neuropharm.2015.05.038.

Small molecule inhibitors of PSD95-nNOS protein-protein interactions as novel analgesics

Wan-Hung Lee[1], **Zhili Xu**[2], **Nicole M. Ashpole**[3], **Andy Hudmon**[3], **Pushkar M. Kulkarni**[4], **Ganesh A. Thakur**[4], **Yvonne Y. Lai**[2], and **Andrea G. Hohmann**[1,2,5,*]

[1]Biochemistry Interdisciplinary Graduate Program, Molecular and Cellular Biochemistry Department, Indiana University, Bloomington, IN

[2]Department of Psychological and Brain Sciences, Indiana University, Bloomington, IN

[3]Department of Biochemistry and Molecular Biology, Indiana University School of Medicine, Indianapolis, IN

[4]Center for Drug Discovery, and Department of Pharmaceutical Sciences, Northeastern University, Boston, MA

[5]Gill Center for Biomolecular Science, Bloomington, IN

Abstract

Aberrant increases in NMDA receptor (NMDAR) signaling contributes to central nervous system sensitization and chronic pain by activating neuronal nitric oxide synthase (nNOS) and generating nitric oxide (NO). Because the scaffolding protein postsynaptic density 95kDA (PSD95) tethers nNOS to NMDARs, the PSD95-nNOS complex represents a therapeutic target. Small molecule inhibitors IC87201 (EC_{5O}: 23.94 μM) and ZL006 (EC_{50}: 12.88 μM) directly inhibited binding of purified PSD95 and nNOS proteins in AlphaScreen without altering binding of PSD95 to ErbB4. Both PSD95-nNOS inhibitors suppressed glutamate-induced cell death with efficacy comparable to MK-801. IC87201 and ZL006 preferentially suppressed phase 2A pain behavior in the formalin test and suppressed allodynia induced by intraplantar complete Freund's adjuvant administration. IC87201 and ZL006 suppressed mechanical and cold allodynia induced by the chemotherapeutic agent paclitaxel (ED_{50}s: 2.47 and 0.93 mg/kg i.p. for IC87201 and ZL006, respectively). Efficacy of PSD95-nNOS disruptors was similar to MK-801. Motor ataxic effects were induced by MK-801 but not by ZL006 or IC87201. Finally, MK-801 produced hyperalgesia in the tail-flick test whereas IC87201 and ZL006 did not alter basal nociceptive thresholds. Our studies establish the utility of using AlphaScreen and purified protein pairs to establish and quantify disruption of protein-protein interactions. Our results demonstrate previously unrecognized antinociceptive efficacy of ZL006 and establish, using two small molecules, a broad application for PSD95-nNOS

[*]**Address for correspondence**: Andrea G. Hohmann, Department of Psychological and Brain Sciences, Indiana University, 1101 E 10th Street, Bloomington, IN 47405-7007, USA. Phone: +1 8128560672, hohmanna@indiana.edu.

Conflict of interest

YYL is currently partly employed at Anagin, LLC.

inhibitors in treating neuropathic and inflammatory pain. Collectively, our results demonstrate that disrupting PSD95-nNOS protein-protein interactions is effective in attenuating pathological pain without producing unwanted side effects (i.e. motor ataxia) associated with NMDAR antagonists.

1. Introduction

Chronic pain is a devastating clinical problem resulting from nerve injury, disease states (e.g. diabetes or cancer) or toxic challenges. It is the most common cause of long-term disability, and fewer than 50% of patients receive adequate pain relief (Steglitz et al., 2012). Alterations in the properties of peripheral nerves by inflammation-associated changes in the chemical environment of the nerve fiber has been implicated in peripheral sensitization (Basbaum et al., 2009). In addition to peripheral mechanisms, central sensitization, a process which establishes hyperexcitability in the central nervous system (CNS), leads to enhanced processing of nociceptive messages, thus contributing to both the development and maintenance of chronic pain (Basbaum et al., 2009). One of the mechanisms involved in central sensitization is through excessive glutamatergic signaling and overactivation of the *N*-methyl-D-aspartate receptor (NMDAR) (Latremoliere and Woolf, 2009; South et al., 2003; Woolf, 1983). Overactivation of NMDARs leads to increased calcium influx in the postsynaptic cell and, consequently, increases downstream signaling events critical for the development and maintenance of chronic pain (Latremoliere and Woolf, 2009). NMDAR antagonists (e.g. ketamine, MK-801, and memantine) produce antinociceptive efficacy in various animal pain models (Zhou et al., 2011); however, direct antagonism of NMDAR produces adverse pharmacological effects (e.g. motor impairment, memory impairment, dissociative effects) due to the broad involvement of NMDAR signaling in numerous physiological functions (Zhou et al., 2011).

We hypothesized that disrupting protein-protein interactions that mediate downstream signaling events critical for pronociceptive NMDAR activation may suppress pain without triggering unwanted side effects mediated by direct antagonism of NMDAR (Florio et al., 2009). NMDAR activation leads to production of nitric oxide (NO), which, when produced in excess, is implicated in pathological processes including inflammation and pain (Miclescu and Gordh, 2009). The production of NO is linked to NMDAR activation through neuronal nitric oxide synthase (nNOS), an enzyme which is tethered to NMDAR by the scaffolding protein postsynaptic density 95 kDA (PSD95) (Christopherson et al., 1999; Luo and Zhu, 2011; Sattler et al., 1999). This NMDAR-PSD95-nNOS complex is required for NMDAR mediated NO production and has thus been implicated in neurological diseases and neuronal excitotoxicity (Courtney et al., 2014; Li et al., 2013; Toro and Deakin, 2005). IC87201 (see Figure 1), the first small molecule disruptor of PSD95-nNOS interaction, produces antinociceptive efficacy following intrathecal administration in a manner mimicked by the fusion protein TAT-nNOS (Florio et al., 2009). ZL006 (see Figure 1) is a second small molecule disruptor of PSD95-nNOS interaction that shows therapeutic efficacy in models of stroke and depression (Doucet et al., 2013; Zhou et al., 2010). Whether ZL006 produces antinociceptive efficacy in models of pathological pain remains unknown. Disruption of the NMDAR-PSD95 complex with a peptide inhibitor, TAT-NR2B9c, also produces antinociception in a model of neuropathic pain induced by traumatic nerve injury (D'Mello

et al., 2011). These observations provide evidence that targeting the NMDAR-PSD95-nNOS complex downstream of NMDAR signaling pathway may be effective in blocking the NMDAR triggered central sensitization. Thus the PSD95-nNOS protein-protein interface represents a potential target for treating pain and other disease states involving aberrant NMDAR signaling.

ZL006 inhibits glutamate-induced cell death and glutamate-induced increases in nNOS-PSD95 protein complex in primary neuronal cells (Zhou et al, 2010). However, it is unclear whether these effects occur through direct disruption of the PSD95-nNOS complex because there is no evidence that ZL006 inhibits this complex *in vitro*. We, therefore, examined the ability of small molecule inhibitors ZL006 and IC87201 to disrupt binding between purified PDZ domains of nNOS and PSD95 using an amplified luminescence proximity homogeneous assay (AlphaScreen). In addition, we characterized the effect of IC87201 and ZL006 on the binding of PSD95 to receptor tyrosine-protein kinase ErbB4 to assess specificity of these inhibitors for disrupting PSD95-nNOS protein-protein interactions. To characterize the cell-based efficacy of these small molecules, we evaluated whether these inhibitors protect cortical neurons from glutamate-induced excitotoxicity. We also characterized the antinociceptive efficacies of these small molecule disruptors in mouse models of inflammatory and neuropathic pain. Intrathecal administration of IC87201 has previously been shown to attenuate both NMDA-induced hyperalgesia and neuropathic pain induced by chronic constriction injury (CCI) (Florio et al., 2009). However, whether IC87201 shows antinociceptive efficacy in chronic pain models following systemic administration remains unknown. Here, we used two small molecule PSD95-nNOS inhibitors to determine whether disruption of PSD95-nNOS interactions produces broad spectrum antinociceptive efficacy in models of inflammatory pain induced by intraplantar administration of either formalin or complete Freund's adjuvant (CFA) administration and neuropathic pain induced by treatment with the chemotherapeutic agent paclitaxel. Our studies provide evidence that ZL006 directly disrupts the PSD95-nNOS complex and provides the first characterization of the antinociceptive efficacy of ZL006 in pain models. Our studies also extend findings of Florio (2009) by evaluating efficacy of IC87201 in models of inflammatory pain and toxic neuropathy and by employing a systemic (i.p.) route of drug administration. The formalin test is a model of tonic inflammatory pain and the second phase of formalin-evoked nociceptive behaviors have been linked to NMDAR-dependent central sensitization (Tjolsen et al., 1992). The CFA model is a pervasive inflammatory pain model which has been linked to activation of nNOS (Chen et al., 2010; Chu et al., 2005). Thus, these two inflammatory pain models were used, together with two small molecule inhibitors (i.e. IC87201 and ZL006) to ascertain whether nNOS-PSD95 inhibitors suppress inflammatory pain. Chemotherapeutic agents, such as paclitaxel, induce peripheral neuropathy in mice and rats, similar to that observed in cancer patients undergoing chemotherapy treatment (Windebank and Grisold, 2008). Thus, we asked whether nNOS-PSD95 inhibitors disrupt mechanical and cold allodynia (Jaggi et al., 2011) induced by paclitaxel treatment in mice. We also employed the tail immersion test to assess whether small molecule inhibitors themselves produce analgesic effects in the absence of a pathological pain state. Comparisons in all studies were made with the NMDAR antagonist MK-801, used as a reference compound. Finally, we compared side-effect profiles of

PSD95-nNOS inhibitors with MK-801 using the rotarod test of motor ataxia. Our studies demonstrate that ZL006, like IC87201, directly disrupts the PSD95-nNOS complex and reveal previously unidentified anti-allodynic properties of ZL006. Our in vivo studies also suggest that IC87201 and ZL006 suppress a broad spectrum of pathological pain states without producing adverse side effects of NMDAR antagonists.

2. Materials and methods

2.1. Protein purification

Glutathione S-transferase (GST) or His-tagged proteins were expressed in *E-Coli*, purified on GST or Nickel columns respectively according to manufacturers' instructions. $PSD95_{1–392}$ containing the PDZ domains that bind nNOS was expressed either as GST- or His-tagged using pGEX 4T-1 or pET-30a respectively. $nNOS_{1–299}$ containing the PDZ domain that binds PSD95, but lacking the catalytic domain, was expressed as His-tagged.

2.2. AlphaScreen assay

AlphaScreen solution binding between nNOS and PSD95 was carried out using purified N-terminal His-$nNOS_{1–299}$ and GST-$PSD95_{1–392}$ proteins according to manufacturer's instructions (PerkinElmer, Waltham, MA). Briefly, purified His-nNOS and GST-PSD95 proteins were incubated for 1 h at room temperature (RT), with gentle shaking. AlphaScreen Ni Chelate Acceptor beads (final 20 μg/ml) and AlphaScreen Glutathione Donor beads (or Streptavidin donor beads for biotinylated ErbB4) (final 20 μg/ml) were sequentially added, with 1 h incubation for each addition. The reaction was carried out in 20–40 μl final volume in 96-well ½ area plates in 1X PBS, 0.1% BSA and 0.05% Tween-20. Plates were read on an EnSpire® Multimode Plate Reader (PerkinElmer, Waltham, MA) equipped with AlphaScreen optical detection module. 50% binding (or Kd) between His-nNOS and GST-PSD95 was determined by titrating both proteins (0–350 nM). To test disruption of the protein-protein complex by small molecule inhibitors, the reaction was carried out using concentrations of His-nNOS and GST-PSD95 at 50% maximum binding. Inhibitors or vehicle (containing equivalent amount of DMSO) were added to the proteins at the beginning of the experiments. All the compounds used in this experiment were prepared as 20 mM stocks dissolved in DMSO and subsequent dilutions were further made from this stock. Control experiments testing the ability of the small molecule inhibitors in disrupting bead interactions were used with recombinant GST-His tag (GenWay Biotech Inc, CA).

2.3. Embryonic cortical neuron culture

Cortical tissue from E18-E19 Sprague-Dawley rat pups was harvested according to approved IACUC guidelines as previously described (Ashpole and Hudmon, 2011; Hudmon et al., 2005). Pelleted cortical cells were resuspended in neuronal growth media (Neurobasal media containing 2% NuSerum (BD Biosciences, San Jose, CA), 2% NS21 (Chen et al., 2008) and penicillin (10 units/mL), streptomycin (10 μg/mL), and L-glutamine (29.2μg/mL) at a density of 2.5 million cells/mL and seeded on poly-D-lysine (50 μg/mL) coated 15mm coverslips (German glass Number 0). Forty-eight hours after plating, cultures were treated with 5-fluor-2'-deoxyuridine (1.5 μg/mL) and uridine (3.5 μg/mL).

2.4. Excitotoxic Stimulation

Neurons (7–8 DIV) were pretreated with the small molecule inhibitors IC87201 (10 μM), ZL006 (10 μM), the NMDAR antagonist MK-801 (20 μM) or vehicle for 20 min at 37°C and subsequently stimulated with 200 μM glutamate/20 μM glycine for 1 h at 37 °C (Ashpole and Hudmon, 2011). Following treatment, stimulation media was washed out with fresh neuronal growth media and the neurons were incubated for 24 h until analysis.

2.5. Cell death assay

Twenty-four hours following excitotoxic stimulation, the coverslips were washed in PBS and stained using Live/Dead Cytotoxicity/Viability kit per manufacturer's recommendation (Molecular Probes, Eugene, OR). Following staining, the coverslips were washed in PBS and immediately imaged on Nikon Ti-E inverted microscope (100X magnification). Each coverslip was imaged in three different fields using a Texas Red filter to detect cytotoxic cells and a FITC filter to detect viable cells. Cells were quantified using the automated counting software Nikon Elements 3.0.

2.6. Animals and housing conditions

Adult C57BL/6J male mice (Jackson Laboratory, Bar Harbor, ME), weighing 23–33g were used in these experiments. Animals were maintained in a temperature-controlled facility (73 ±2°F, 45% humidity, 12-hour light/dark cycle) with food and water *ad libitum*. All experimental procedures were approved by Bloomington Institutional Animal Care and Use Committee of Indiana University and followed guidelines of the International Association for the Study of Pain.

2.7. Drugs and chemicals

ZL006 and IC87201 were synthesized for our studies by the METACyt facility (Indiana University, Bloomington) and subsequently in the laboratory of Dr. Ganesh Thakur, (by P.M.K) at Northeastern University Center for Drug Discovery (Boston, MA). MK-801 was purchased from Sigma Aldrich (St. Louis, MO). All drugs were dissolved in 3% DMSO, 1:1:18 of emulphor (Alkamuls EL 620L; Solvay): ethanol (Sigma-Aldrich): 0.9% NaCl (Aquilite System; Hospira, Inc, Lake Forest, IL).

2.8. Formalin test

Animals were injected intraperitoneally (i.p.) with IC87201 (4 or 10 mg/kg, i.p.), ZL006 (4 or 10 mg/kg, i.p.), MK-801 (0.1 mg/kg, i.p.) or vehicle thirty minutes prior to intraplantar (i.pl.) injection of formalin. Animals were placed in an elevated clear observation chamber immediately after injection. Thirty minutes after injection, animals were injected (10 μl) unilaterally into the plantar surface of the right hind paw with 2% formalin (37% formaldehyde diluted in 0.9% NaCl). Resulting nociceptive behaviors were scored for forty minutes immediately following formalin injection. Composite pain scores were calculated for every 5 minute bin for a total duration of 40 min using the following scoring criteria: no behavior was scored 0, lifting was scored 1, and shaking/biting/flinching was scored as 2. Pain behavior was separated into the early phase (phase 1) and late phase (phase 2A and phase 2B) of pain behavior, similar to that described previously (Malmberg and Yaksh,

1992; Tjolsen et al., 1992).The area under the curve of pain behavior was calculated for Phase 1 (0–10 min), phase 2A (10–20 min) and phase 2B (20–40 min) for each subject and subjected to statistical analysis.

2.9. Paclitaxel-induced neuropathy

Paclitaxel (Tecoland Corporation, Irvine, CA) was dissolved in a vehicle consisting of a 1:1:4 ratio of cremophor EL (Sigma-Aldrich, St. Louis, MO)/ethanol (Sigma-Aldrich) saline (Aquilite System; Hospira, Inc, Lake Forest, IL). Animals were injected with either the cremophor-vehicle or paclitaxel (4 mg/kg, i.p.) on day 0, 2, 4, and 6 following initiation of paclitaxel dosing (16 mg/kg i.p. cumulative dose). Baseline (day 0) responding to mechanical stimulation was assessed before initiation of paclitaxel (or vehicle) dosing. Responsiveness to mechanical stimulation was also assessed during development and maintenance phases of paclitaxel-induced hypersensitivity on days 4, 7, 11 and 15.

2.10. Dose response of PSD95-nNOS inhibitors in paclitaxel induced neuropathy model

When paclitaxel induced neuropathy was stable (i.e. beginning on day 16 post initiation of paclitaxel dosing), mice were injected with IC87201 (0.1, 0.3, 1, 3, 10, and 30 mg/kg i.p, respectively), ZL006 (0.1, 0.3, 1, 3, 10, and 30 mg/kg i.p, respectively) or vehicle every three days using a within subjects dosing paradigm. Pre-injection baselines were measured prior to each injection day, ensuring that the mechanical and cold responsiveness returned to baseline, without any carry over effects, prior to dose escalation. Responsiveness to mechanical and cold stimulation was assessed 30 min after drug or vehicle injection to calculate ED50s for suppressing paclitaxel-induced mechanical and cold allodynia.

2.11. Time course of suppression of paclitaxel-induced allodynia by PSD95-nNOS inhibitors and comparison to MK-801

In a separate study, we established the time course of anti-allodynic efficacy of PSD95-nNOS inhibitors on paclitaxel-induced mechanical allodynia using the maximally effective doses of PSD95-nNOS disruptors identified in the dose response study described above. Mice were treated with either paclitaxel or cremophor-vehicle as described above. On day 16 following initiation of paclitaxel (or cremophor vehicle) dosing, mice received a single i.p. injection of IC87201 (10 mg/kg, i.p.), ZL006 (10 mg/kg, i.p.), MK-801 (0.1 mg/kg, i.p.) or vehicle. Responsiveness to mechanical stimulation was assessed before pharmacological manipulations (pre drug post paclitaxel baseline) and then reassessed at 30, 90, and 150 minutes after drug injection.

2.12. Complete Freund’s adjuvant (CFA) induced inflammatory pain

Mice received a single intraplantar (20 μl i.pl.) injection of complete Freund’s adjuvant (CFA; Sigma-Aldrich, St. Louis, MO) diluted with saline in a 1:1 ratio in the right hind paw. Mechanical thresholds that elicited paw withdrawal were assessed with an electronic von Frey anesthesiometer (IITC Life Science, Woodland Hills, CA). Thresholds were assessed prior to CFA injection (baseline) and 48 hours after CFA administration (pre drug baseline). Mice were then treated with IC87201 (10 mg/kg, i.p), ZL006 (10 mg/kg, i.p), MK-801 (0.1

mg/kg, i.p) or vehicle and responsiveness to mechanical stimulation was reassessed again at 30, 90, and 150 minutes after pharmacological manipulations.

2.13. Assessment of mechanical allodynia

Withdrawal thresholds (g) to mechanical stimulation were measured in duplicate for each paw using an electronic von Frey anesthesiometer supplied with a 90-g semi-flexible probe (IITC Life Science, Woodland Hills, CA) as described previously (Deng et al., 2015; Guindon et al., 2013).

2.14. Assessment of cold allodynia

Cold allodynia was assessed by applying acetone (Sigma Aldrich, St. Louis, MO) to the plantar surface of the hind paw. Time spent reacting to acetone stimulation was measured in triplicate for each paw (Deng et al., 2015; Ward et al., 2011).

2.15. Rota-rod test

Motor performance was assessed using an accelerating Rota-rod (IITC Life Science) (4–40 rpm with cutoff time of 300 sec). Mice were trained for two days and on the third day, the baseline descent latency was measured. On the fourth day, the mice were injected with IC87201 (10 mg/kg, i.p.), ZL006 (10 mg/kg, i.p.), MK-801 (1 mg/kg, i.p.) or vehicle. Thirty minutes after the injection, the mice were placed on the accelerating rod and the latency for the animals to stay on the rod was recorded. On the baseline and post-drug test day, the animal must pass a criterion in order to advance to assessment of drug effects. Animals that did not pass criteria (i.e. ability to walk on rotating drum for 30 sec) did not receive pharmacological manipulations.

2.16. Effects of supramaximal doses in tail-flick test of analgesia and rota-rod test of motor ataxia

To ascertain whether PSD95-nNOS inhibitors (i.p.) produce antinociception in the absence of pathological pain, we evaluated PSD95-nNOS inhibitors in the tail-flick test at doses that were three times higher than the maximally effective anti-allodynic doses identified in our studies. We also evaluated the possible side effect profile of these supra-maximal doses in the rota-rod test using the same animals. Mice were trained in the rota rod test on two days prior to establishment of the tail flick baseline. Baseline tail flick latency was measured by immersing one half to two thirds of the tail into 53–54°C of warm water. The latency for an animal to remove its tail from the water was measured three times prior to pharmacological manipulations. Mice received IC87201 (30 mg/kg, i.p), ZL006 (30 mg/kg, i.p), MK-801 (0.3 mg/kg, i.p) or vehicle. Tail flick latency was measured again 30 min after drug or vehicle administration. Immediately after determination of post-injection tail-flick latencies, the latency for animals to fall of the rota-rod was again recorded in duplicate.

2.17. Statistical Analysis and ED_{50} calculation

IC_{50} or EC_{50} values in AlphaScreen were calculated by non-linear regression analysis using the equation of a sigmoid concentration-response curve (GraphPad Prism). The following formula was used to calculate %MPE: (Post paclitaxel post drug response - Post paclitaxel

pre drug response)/(Pre paclitaxel baseline - Post paclitaxel pre drug response) × 100. ED_{50} was then determined by the equation of non-linear regression for log (inhibition) versus response curve (GraphPad Prism). Impact of PSD95-nNOS inhibitors and MK-801 on glutamate-induced cell death was analyzed by one way ANOVA followed by Bonferroni post hoc tests. *In vivo* data were analyzed by repeated measures and one-way ANOVA, as appropriate. The area under the curve (AUC) of pain behavior was calculated for phase 1, phase 2A and phase 2B and ANOVA was performed on each phase separately. Analysis of variance for repeated measures was used to determine the time course of drug effects. One-way ANOVA was then used to identify the time points during which group differences attributable to significant interactions were observed. Bonferroni was used for *post hoc* tests. All statistical analyses were performed using IBM-SPSS Statistics version 22.0 (SPSS inc., an IBM company, Chicago, IL, USA). $p<0.05$ was considered statistically significant.

3. Results

3.1. Small molecules, IC87201 and ZL006, inhibit PSD95-nNOS protein-protein interactions *in vitro*

IC87201 was first identified from a high-throughput screen as a PSD95-nNOS inhibitor using an *in vitro* plate binding assay (Florio et al., 2009), but *in vitro* data documenting disruption of PSD95-nNOS binding by ZL006 has never been reported. We, therefore, developed *in vitro* protein-protein interaction solution binding assays using AlphaScreen to detect the complex of the PDZ domains of PSD95 and nNOS and disruption by small molecules (Figure 2). N-terminal His-$nNOS_{1–299}$ and GST-$PSD95_{1–392}$ were bound to Ni-chelate acceptor beads and Glutathione-donor beads respectively. Saturation binding between His-$nNOS_{1–299}$ and GST-$PSD95_{1–392}$ using increasing concentrations (0–350 nM) of both proteins showed that the proteins bind with an EC_{50} of 30 nM in an AlphaScreen assay (Figure 2A; consistent with data published previously in (Harris et al., 2001; Tochio et al., 2000)). $nNOS_{1–130}$ without any tag competed effectively with nNOS-PSD95 interaction with IC_{50} of 30 nM (data not shown) similar to Kd of the binding. Small molecule inhibitors IC87201 and ZL006 inhibited the interaction between GST-$PSD95_{1–392}$ and His-$nNOS_{1–299}$ (Figure 2B) with IC_{50} of 23.94 ± 9.89 μM (n = 7) and 12.88 ± 4.14 μM (n = 7), respectively. As a control, we used a protein containing both GST-His tags to measure interaction between Ni-chelate acceptor and Glutathione-donor beads. IC87201 and ZL006 did not inhibit the acceptor-donor bead interaction in an AlphaScreen binding assay using this recombinant GST-His control protein (data not shown).

3.2. IC87201 and ZL006 do not disrupt ErbB4-PSD95 interactions

To investigate whether these small molecule PSD95-nNOS inhibitors disrupt other PDZ-PDZ protein interactions, we characterized related protein-protein interactions involving PDZ domains of nNOS and ErbB4. The PDZ2 domain of PSD95 interacts with the receptor tyrosine-protein kinase ErbB4 (Garcia et al., 2000; Huang et al., 2000) In our AlphaScreen binding assay, the biotinylated C-terminal tail of ErbB4 (amino acid1289–1308) interacts with a His fusion protein containing the PDZ1–3 domain of PSD95 with an apparent affinity of 10 nM (Figure 2C). IC87201 and ZL006 (up to 150 μM) had no effect on the interaction between ErbB4 and PSD95 (n = 2; Figure 2D).

3.3. Glutamate-induced excitotoxicity is antagonized by IC87201 and ZL006

The ability of the PSD95-nNOS inhibitors to protect neurons from excitotoxic death was examined in cultured cortical neurons subjected to glutamate (200 μM)/glycine (20 μM) for 1 h. Glutamate/glycine induces cell death in primary cortical neurons [$p < 0.0001$] pre-treated with vehicle relative to the control level (no glu/gly). However, glutamate-induced neuronal death was attenuated in cortical neurons pretreated with either IC87201 (10 μM), ZL006 (10 μM), or the NMDAR antagonist MK-801 (20 μM) [$p < 0.001$ for all comparisons] relative to glu/gly treatment in neurons pre-treated with vehicle (Figure 3). Cell death in IC87201, ZL006, and MK-801 conditions did not differ from each other and was normalized relative to control levels (Figure 3).

3.4. Small molecule PSD95-nNOS inhibitors attenuate formalin-induced pain behaviors

Intraplantar formalin (2% in10 μl) induced time dependent changes in pain related behaviors in all studies [$p < 0.001$ ANOVA]. The high dose of IC87201 (10 mg/kg i.p.) suppressed composite pain scores relative to vehicle [$F_{1,13} = 7.727$, $p < 0.001$] and these effects were time dependent [$F_{8,144} = 2.775$, $p = 0.008$] (Figure 4A). The low dose of IC87201 did not reliably suppress formalin-induced pain behavior, although antinociceptive effects of the high and low doses did not differ over the entire observation interval (Figure 4A). The high dose of IC87201 preferentially suppressed the AUC of formalin-induced pain behavior relative to vehicle during phase 2A [$p < 0.05$, bonferroni] but not during phase 2B [$p = 0.307$] or phase 1 [$p = 0.94$] (Figure 4B).

ZL006 attenuated formalin-induced pain behavior [$F_{2,17} = 13.067$, $p < 0.0004$, ANOVA] relative to vehicle treatment and these effects were time dependent [$F_{16,136} = 2.877$, $p < 0.0005$] (Figure 4C). Both doses of ZL006 suppressed phase 1 pain behavior in comparison to the vehicle-treated group (Figure 4C) [$p < 0.01$, at 4 and 10 mg/kg, bonferroni]. Post hoc analysis revealed that the high dose of ZL006 suppressed formalin-evoked pain behavior from 15–20 min [$p < 0.01$ for each comparison, bonferroni] following injection whereas the low dose suppressed pain at 15 min only [$p < 0.05$, bonferroni]. Similarly, both doses of ZL006 reduced the AUC of pain behavior relative to vehicle treatment during both phase 1[$p < 0.01$ for both doses, bonferroni] and phase 2A [$p < 0.05$ for 4 mg/kg; $p < 0.01$ for 10 mg/kg] but not phase 2B (Figure 4D).

We compared effects of efficacious doses of PSD95-nNOS inhibitors with the NMDAR antagonist MK-801 in the formalin test. The experimental treatments suppressed composite pain scores [$F_{3,23} = 12.251$, $p < 0.00006$] and these effects were time dependent [$F_{3,21} = 5.912$, $p < 0.005$] (Figure 4E). Post hoc analyses revealed that both ZL006 and MK-801 suppressed composite pain scores during phase 1 (5 min post formalin injection) and from 15–20 min post formalin ($p < 0.001$), whereas antinociceptive effects of IC87201 were reliable at 20 min only ($p = 0.002$) (Figure 4E). Both MK-801 and ZL006 reduced AUC of pain behavior during phase 1 and phase 2A relative to the vehicle group (Figure 4F) [phase 1: $p < 0.01$ ZL006, $p < 0.001$ MK-801; phase 2A: $p < 0.001$ ZL006, $p < 0.001$ MK-801, bonferroni], whereas IC87201 reduced AUC of pain behavior during phase 2A only (Figure 4F) [$p < 0.05$, bonferroni] without reliably altering pain behavior during phase 1 or phase 2b [$p > 0.064$ for each comparison].

3.5. Small molecule PSD95-nNOS inhibitors suppress mechanical allodynia induced by complete Freund's adjuvant

The baseline mechanical threshold did not differ between the two hind paws prior to CFA injection [p = 0.305, independent sample t-test]. CFA decreased mechanical paw withdrawal thresholds in the paw ipsilateral [p < 0.005, paired sample t-test] but not contralateral to CFA injection. The small molecule inhibitors elevated paw withdrawal thresholds relative to pre-treatment thresholds [$F_{3,60}$ = 20.535; p = 0.017] (Figure 5A).

Both IC87201 [p < 0.003, bonferroni] and ZL006 [p < 0.002, bonferroni], at doses of 10 mg/kg i.p., suppressed mechanical allodynia starting at 30 min post injection relative to vehicle. Both small molecules normalized mechanical paw withdrawal thresholds to pre-CFA levels [p = 0.216 at 30 min IC87201; p = 0.283 at 30 min ZL006 two tailed paired sample t-test]] (Figure 5A). Similarly, MK-801 (0.1 mg/kg, i.p.) suppressed CFA-induced mechanical allodynia relative to vehicle [p < 0.009, 30 min post injection; bonferroni] and normalized paw withdrawal thresholds to pre-CFA baseline levels [p = 0.283 at 30 min, 2 tailed paired sample t-test] (Figure 5A). However, anti-allodynic efficacy was no longer present 90 min following any treatment [p = 0.962, MK-801 bonferroni; p = 1.00, IC87201; p = 1.00, ZL006]. Mechanical paw withdrawal thresholds did not differ in the paw contralateral to CFA injection in any group [$F_{3,20}$ = 2.549, p = 0.085] or at any time point [$F_{9,60}$ = 0.524, p = 0.852] (Figure 5B).

3.6. Dose response of small molecule inhibitors in paclitaxel-induced neuropathy pain model

Paclitaxel produced mechanical and cold allodynia relative to pre-paclitaxel baseline responsiveness [p < 0.007 mechanical; p < 0.002 cold, paired sample t-test] (Figure 6A–F). Both mechanical and cold allodynia were assessed prior to every pharmacological treatment in mice used to calculate within subjects dose response curves; no residual drug effects were observed in either mechanical [$F_{2,15}$ = 0.774, p = 0.479; Figure 6A] or cold [$F_{2,15}$ = 0.17, p = 0.846; Figure 6B] responsiveness during the maintenance phase of paclixel-induced allodynia, assessed prior to subsequent dose escalations.

IC87201 and ZL006 attenuated established paclitaxel-induced mechanical allodynia [$F_{2,15}$ =12.562; p = 0.001] relative to vehicle treatment [p < 0.04, bonferroni] at doses (i.p.) of 3 mg/kg [p = 0.033 IC87201; p = 0.006 ZL006, bonferroni], 10 mg/kg [p = 0.001 IC87201; p < 0.001 ZL006, bonferroni] and 30 mg/kg [p < 0.001 IC87201; p < 0.001 ZL006, bonferroni] (Figure 6C). Post injection mechanical paw withdrawal thresholds were also normalized to baseline (pre-paclitaxel) thresholds at doses of 3 mg/kg [p = 0.245 IC87201; p = 0.273 ZL006, paired sample t-test] and 10 mg/kg i.p. [p = 0.634 IC87201; p = 0.975 ZL006, paired sample t-test] (Figure 6C). Similarly, IC87201 and ZL006 also attenuated cold allodynia provoked by paclitaxel treatment at doses of 10 mg/kg [p = 0.002 IC87201; p < 0.001 ZL006, bonferroni] and 30 mg/kg i.p. [p = 0.004 IC87201; p = 0.002 ZL006, bonferroni] relative to vehicle treatment (Figure 6D). Responsiveness to cold was normalized to baseline pre-paclitaxel responsiveness at a dose of 10 mg/kg for ZL006 [p = 0.38, paired sample t-test] (Figure 6D). The dose response relationship of IC87201 and ZL006 in suppressing allodynia was further plotted as % maximal possible effect (%MPE)

and ED_{50} were determined with non-linear regression curves. The ED_{50} for suppression of mechanical allodynia was 2.47 ± 1.3 mg/kg, i.p. for IC87201 and 0.93 ± 0.43 mg/kg, i.p. for ZL006 (Figure 6E). The ED_{50} for suppression of cold allodynia was 1.6 ± 0.33 mg/kg, i.p. for IC87201 and 3.7 ± 0.54 mg/kg, i.p. for ZL006 (Figure 6F). The ED_{50} determined for suppression of mechanical allodynia did not differ between the two small molecule inhibitors [p = 0.266]. However, the ED_{50} for suppression of cold allodynia was lower for ZL006 compared to IC87201 [p < 0.002; independent sample t-test, two tailed].

3.7. Time course of suppression of paclitaxel-induced allodynia induced by nNOS-PSD95 inhibitors and comparison with MK-801

We evaluated the time course of anti-allodynic efficacy of maximally effective doses of PSD95-nNOS inhibitors in mice treated with either paclitaxel or its cremophor-based vehicle. There were no differences between groups in mechanical paw withdrawal thresholds prior to administration of paclitaxel or cremophor vehicle [p = 0.589, one way anova]. Paclitaxel decreased mechanical paw withdrawal thresholds [$F_{1,46}$ = 58.702; p < 0.001] relative to the cremophor-treated group [p < 0.006, one-way anova] prior to drug treatments, consistent with the development of mechanical allodynia (Figure 7A). Mechanical allodynia was maintained from day 4 to day 15 in paclitaxel-treated group relative to day 0 pre-paclitaxel baseline responding [$F_{4,184}$ = 5.94, p < 0.0002] prior to drug manipulations (Figure 6A).

Small molecule PSD95-nNOS inhibitors (10 mg/kg i.p.) attenuated paclitaxel-induced mechanical allodynia [$F_{3,20}$ = 4.46; p < 0.02] relative to vehicle [p < 0.05, bonferroni] and pre-injection levels [$F_{9,60}$ = 2.305; p = 0.036] (Figure 7B). This pattern of suppression was similar to that produced by the NMDAR antagonist MK-801. MK-801 (0.1 mg/kg i.p.) similarly suppressed paclitaxel-induced mechanical allodynia relative to vehicle [p < 0.05, bonferroni] from 30 to 90 min post injection (Figure 7B) and normalized paw withdrawal thresholds to pre-paclitaxel baseline levels [p = 0.662 at 30 min; p = 0.103 at 90 min, 2 tailed paired sample t-test]. Similarly, both IC87201 [p < 0.02, bonferroni] and ZL006 [p < 0.05, bonferroni] suppressed mechanical allodynia starting at 90 min post injection relative to vehicle and normalized thresholds to pre-paclitaxel levels [p = 0.215 at 90 min IC87201; p = 0.15 at 90 min ZL006 two tailed paired sample t-test] (Figure 6B). Anti-allodynic efficacy was no longer present 150 min following injection after any treatment [p > 0.299]. Moreover, in cremophor vehicle-treated mice, MK-801, IC87201 and ZL006 did not alter mechanical withdrawal thresholds [$F_{3,20}$ = 0.437, p = 0.729] or produce antinociception at any time point [$F_{12,80}$ = 0.623, p = 0.817] (Figure 7C).

3.8. Small molecule PSD95-nNOS inhibitors do not produce motor ataxia at efficacious doses

Neither IC87201 nor ZL006, administered at anti-allodynic doses (10 mg/kg, i.p), produced motor ataxia in the rota-rod test (Figure 8) [$F_{4,31}$ = 2.124, p = 0.101]. A high dose (1 mg/kg i.p.) but not the low dose (0.1 mg/kg i.p.) of MK-801 impaired motor coordination relative to the vehicle-treated group (Figure 8) [p < 0.003, bonferroni].

3.9. Supramaximal doses of small molecule PSD95-nNOS inhibitors do not produce analgesia in tail-flick test or motor ataxia

Supra-maximal doses (30 mg/kg i.p.) of IC87201 and ZL006, administered at three times the maximal anti-allodynic dose, did not alter tail-flick latencies in otherwise naïve animals [$F_{3,20}$ = 1.326, p = 0.294] (Figure 9A). MK-801 (0.3 mg/kg i.p) produced hyperalgesia relative to the vehicle group under identical conditions [p = 0.035, bonferroni] (Figure 9A). Motor ataxia was not observed in the rota-rod test in the same mice treated with either IC87201 or ZL006 (30 mg/kg, i.p.) (Figure 9B) [$F_{3,20}$ = 2.721, p = 0.072]. Motor coordination was significantly impaired relative to vehicle in MK801-treated mice (0.3 mg/kg i.p.) under analogous conditions [p < 0.001, bonferroni].

4. Discussion

Our studies provide evidence that two small molecule protein-protein interaction inhibitors, IC87201 and ZL006, disrupt binding of purified nNOS and PSD95 proteins *in vitro*, protect against glutamate-induced excitotoxicity in cortical neurons and produce antinociceptive effects similar to the NMDAR antagonist MK-801. Strikingly, motor ataxic effects associated with NMDAR blockade were absent at therapeutically efficacious doses of nNOS-PSD95 inhibitors and doses three times higher than the maximal anti-allodynic doses of these agents. NMDAR activation induces NO production by nNOS; this signaling cascade is critically involved in central sensitization, a process which underlies the development and maintenance of pathological pain (Latremoliere and Woolf, 2009). PSD95 tethers nNOS to NMDAR, serving a key linking NO production to NMDAR activation. IC87201, the first in class PSD95-nNOS small molecule inhibitor disrupted PSD95-nNOS interaction in a plate binding assay and attenuated the NMDA-induced increases in cGMP production in primary hippocampal neurons *in vitro* (Florio et al., 2009). These findings suggest that NO production downstream of NMDAR activation is inhibited by PSD95-nNOS disruption with IC87201. Similarly, ZL006, a related chemical analog of IC87201 identified by Zhou and colleagues, was shown to reduce PSD95-nNOS association in neurons treated with Glu-Gly (Zhou et al, 2010), although it is unclear whether these effects could be attributed to direct disruption of PSD95-nNOS binding. In this latter study, ZL006 also inhibited NMDAR-dependent NO synthesis (Zhou et al, 2010). The above studies suggest that disruption of PSD95-nNOS interactions reduces NMDAR activation-induced NO production. We, therefore, evaluated whether disruption of PSD95-nNOS protein-protein interactions represents a potential therapeutic strategy for treating inflammatory and neuropathic pain. IC87201 has been shown to attenuate NMDA-induced heat hyperalgesia in mice and mechanical allodynia induced by chronic constriction injury (CCI) in rats following intrathecal administration (Florio et al, 2009). Whether the *in vivo* actions of IC87201 are mediated by PSD95-nNOS disruption or other as yet uncharacterized effects of this molecule remain unknown. We, therefore, chose to evaluate whether ZL006 and IC87201 show a similar pattern of efficacy in disrupting both PSD95-nNOS binding and glutamate-induced cell death *in vitro* and in producing antinociception *in vivo*.

We used AlphaScreen technology to evaluate the ability of IC87201 and ZL006 to disrupt PSD95-nNOS interactions through a direct mechanism *in vitro*. Our studies, using pairs of

purified proteins, demonstrate beyond doubt that IC87201 and ZL006 disrupt PSD95-nNOS interactions. These observations are consistent with the hypothesis that these small molecule act through a direct mechanism to inhibit association of nNOS with PSD95. The observations from our biochemical assay are important because feedforward/feedback loops in more complex cellular systems such as neuronal cells could influence PSD95-nNOS interactions through indirect mechanisms. Our studies are consistent with prior conclusions of the potential mechanisms of action of these small molecules (Florio et al, 2009; Zhou et al 2010) using different methodologies. The specificity of IC87201 is suggested by the failure of IC87201 to disrupt interactions between PSD95-Cypin *in vitro* (cytosolic regulator of PSD95 postsynaptic targeting) (Florio et al, 2009). ZL006 disrupts PSD95-nNOS co-immunoprecipitation in ischemic cortexes but not co-immunoprecipitation of PSD95-SynGAP (synaptic GTPase activating protein) or nNOS-CAPON (carboxyl-terminal PDZ ligand of nNOS) (Zhou et al, 2010). To assess specificity of the presumed biochemical mechanism of these inhibitors, we tested the ability of our small molecules to disrupt another PSD95-interacting partner, ErbB4, because PDZ1 and PDZ2 of PSD95 are known to interact with ErbB4 (Garcia et al., 2000; Huang et al., 2000). Our results show that both IC87201 and ZL006 specifically disrupt PSD95-nNOS through a direct mechanism but do not disrupt PSD95-ErbB4 interactions.

ZL006 pretreatment inhibits NMDAR-dependent excitotoxicity induced by glutamate-glycine treatment (Zhou et al., 2010). Similarly, we pre-treated cortical neuronal cells with either IC87201 or ZL006 (at 10 μM concentrations) and challenged the cells with glutamate/glycine. Our results verify that small molecule inhibitors protect against NMDAR activation-mediated cell death, consistent with the previous findings using ZL006 (Zhou et al., 2010). Note that the concentrations used in the cell death assay reaches nearly complete protection, however, the concentrations used in this study is lower than the IC_{50} determined with AlphaScreen. This inconsistency could be explained by the fact that in biochemical binding assays employing purified proteins more proteins needed to be disrupted in order to calculate a 50% inhibition compared to the native state. In the cell-based assay, it is possible that protective effects can be observed with smaller magnitudes of disruption of the protein complex. Collectively, the data above extend the results of our AlphaScreen binding assays by demonstrating that both IC87201 and ZL006 penetrate cells to disrupt glutamate-dependent signaling and also suggest that disruption of nNOS interaction with PSD95 contributes to excitotoxic cell death. Therefore, disrupting PSD95-nNOS interactions protects neurons from excitotoxic injury. In addition, ZL006 did not inhibit excitatory postsynaptic currents of NMDAR (Zhou et al., 2010); therefore, attenuation of excitotoxicity was not likely due to direct inhibition of Ca^{2+} entry. IC87201 also attenuates NMDA-induced heat hyperalgesia (Florio et al, 2009), suggesting that NMDAR-activated downstream signaling is disrupted *in vivo* to produce antinociception.

Our studies demonstrate, for the first time, that the small molecule PSD95-nNOS inhibitor ZL006 produces antinociception in animal pain models. We also asked whether IC87201 and ZL006 exhibit broad spectrum analgesic efficacy in models of inflammatory and neuropathic pain. Thus, it is noteworthy that both small molecules showed antinociceptive efficacy in inflammatory and neuropathic pain models, including a model of chemotherapy-

induced neuropathy induced by paclitaxel. Thus, anti-allodynic efficacy of IC87201 is observed following systemic drug administration and is not restricted to models of traumatic nerve injury (Florio et al, 2009). Peripheral nerve injury models such as CCI and toxic chemotherapy-induced neuropathy have different underlying mechanisms. Traumatic nerve injury induced by CCI evokes microgliosis, which is evident by microglia activation at the injury site (Calvo and Bennett, 2012). On the other hand, chemotherapy-induced neuropathic pain, such as that induced by paclitaxel, involves distal axonal injury and partial degeneration of the intraepidermal nerve fibers without changing microglial morphology and accumulation during the maintenance of allodynia (Zheng et al., 2011). Astrogliosis and downregulation of glial glutamate transporters GLAST and GLT-1 also contribute to paclitaxel-induced neuropathic pain (Zhang et al., 2012). Therefore, small molecule PSD95-nNOS disruptors show promise for treating a broad spectrum of neuropathic pain states induced by traumatic nerve injury and toxic challenges.

Both IC87201 and ZL006 attenuated formalin pain behavior preferentially during phase 2A. Whereas phase 1 of formalin pain reflects primary afferent activation, phase 2 is specifically linked to central sensitization involving NMDAR activation (Tjolsen et al., 1992) but also involves continued activity in primary afferent fibers; this may partially explain the behavioral differences in 2A and 2B responding (Kaneko and Hammond, 1997). Thus, PSD95-nNOS disruptors may be maximally efficacious during development of central sensitization when MK-801 is also most efficacious. GABA activity diminishes the magnitude of pain behaviors in phase 2A and could possibly limit the development of central sensitization in the spinal cord (Kaneko and Hammond, 1997). This may also explain why the antinociceptive efficacy of both small molecule inhibitors is more profound in phase 2A compared to 2B; inhibitory effects of GABA in phase 2A are enhanced when NMDAR-dependent glutamate signaling is suppressed by PSD95-nNOS disruption.

Interestingly, ZL006, like MK-801, also attenuated nociceptive behaviors during phase 1, which may involve direct chemical activation of primary afferent fibers (Abbadie et al., 1997). ZL006 was also a more potent antinociceptive agent in this formalin pain model relative to IC87201. More work is necessary to determine why IC87201 and ZL006 produced differential effects on phase 1 of formalin pain behaviors. ZL006 also exhibited a lower IC_{50} for disrupting PSD95-nNOS binding in our biochemical AlphaScreen assay.

The CFA model is an inflammatory pain model linked to the activation of nNOS (Chen et al., 2010; Chu et al., 2005). Our results show that both IC87201 and ZL006 were as efficacious as MK-801 in attenuating CFA -induced mechanical allodynia. These small molecule inhibitors may abolish the CFA-induced increased nNOS activity by disrupting PSD95-nNOS interaction as the association of NMDAR-PSD95-nNOS is necessary for nNOS activation (Rameau et al., 2004).

PSD95-nNOS inhibitors did not alter basal nociceptive thresholds in the absence of pathological pain and also failed to produce motor ataxic effects associated with NMDAR antagonists. Doses of small molecule PSD95-nNOS inhibitors that suppressed mechanical allodynia induced by either paclitaxel or CFA and also produced antinociception in the formalin test did not alter mechanical thresholds in mice that did not receive paclitaxel.

Moreover supramaximal doses of IC87201 and ZL006 did not produce analgesia or hyperalgesia in the tail flick test in otherwise naïve mice. Thus, the agents normalized sensitization induced by inflammatory and neuropathic pain to pre-injury levels without producing analgesia. The tail flick assay also revealed that MK-801 produced hyperalgesia under these conditions, whereas IC87201 and ZL006 did not alter basal nociceptive thresholds. This observation is consistent with previous studies in rats demonstrating that acute systemic MK-801 treatment induced mechanical and heat hyperalgesia; this hyperalgesic effect may be associated with increased substance P (SP) and decreased neuropeptides enkephalin (Enk) efficiency (Al-Amin et al., 2003; Schmidt et al., 2009). More work is needed to determine whether small molecules themselves also fail to disturb the levels of these neuropeptides.

We generated dose response curves to calculate the ED_{50} for IC87201 and ZL006 to suppress mechanical and cold allodynia in the paclitaxel model. The ED_{50} of the small molecules did not differ in their ability to suppress mechanical allodynia whereas the ED_{50} for ZL006 was lower than that for IC87201 for suppression of cold allodynia. It is important to note, however, that our studies failed to identify a systemic dose of PSD95-nNOS inhibitors that produced motor impairment (but see (Florio et al., 2009)). Antinociceptive doses of PSD95-nNOS inhibitors up to 30 mg/kg (i.p) failed to produce any observable sign of motor impairment, whereas profound motor ataxia was observed at a dose of 0.3 mg/kg i.p. of MK-801 in the rota-rod test. Thus, although the ED_{50} for the small molecule PSD95-nNOS inhibitors may be higher than that observed for systemically administered MK-801 for suppressing allodynia (e.g. $ED_{50s:}$ 0.15 mg/kg i.p (capsaicin model; (Amador et al., 2001)); 0.01mg/kg i.p. (formalin model (Berrino et al., 2003)), PSD95-nNOS inhibitors clearly exhibit more favorable therapeutic ratios compared to NMDAR antagonists.

Antinociceptive effects of PSD95-nNOS inhibitors are not due to nonspecific disruption of motor function by the small molecules. The rotarod results, in conjunction with the ED_{50} for anti-allodynic efficacy determined in paclitaxel model, suggest that PSD95-nNOS small molecules inhibitors have a wider therapeutic window compared to MK-801 (complete immobility at 0.3 mg/kg i.p.). Thus, PSD95-nNOS disruptors are likely to exhibit favorable therapeutic ratios compared to NMDAR antagonists. Moreover, ZL006, unlike the nNOS inhibitor, 7-nitroindazole (7-NI), did not alter the acquisition of a spatial water maze task nor did it produce aggressive behaviors (Zhou et al., 2010). Thus, other side effect profiles (e.g. memory impairment) of NMDAR antagonists that were not measured in the present study may also be spared by PSD95-nNOS inhibitors.

In summary, we show that IC87201 and ZL006 specifically disrupt PSD95 and nNOS interactions through a direct mechanism. Both small molecules disrupt glutamate-induced neuronal cell death *in vitro* and suppress inflammatory and neuropathic pain *in vivo*. These studies identify previously unrecognized antinociceptive effects of ZL006 using models of inflammatory and neuropathic pain, suggesting that antinociceptive efficacy was likely due to disruption of NMDAR-dependent nNOS signaling pathway. We further show that a broad profile of antinociceptive efficacy of PSD95-nNOS inhibitors is observed following systemic administration in inflammatory pain models and a clinically relevant model of chemotherapy-induced toxic neuropathy. Moreover, PSD95-nNOS inhibitors suppressed

hypersensitivity in pathological pain states without altering basal nociceptive thresholds in the absence of the inflammatory or neuropathic pain state. Collectively, our findings suggest that disruption of PSD95-nNOS with small molecule inhibitors represents a valuable therapeutic strategy for suppressing pathological pain without unwanted side effects associated with NMDAR antagonism. The present studies support a therapeutic strategy of bypassing NMDAR inhibition by targeting downstream protein-protein interactions to suppress pain sensitization without producing NMDAR-associated side effects.

Acknowledgements

We thank Michael Courtney for providing $nNOS_{1–130}$ cleaved from GST-$nNOS_{1–130}$ (University of Eastern Finland, Kuoppio) and Dr. Cary Lai from Indiana University, Bloomington, IN for providing Biot-ErbB4. This work was supported by DA037673 (to AGH and YYL), ICTSI TR000006 (to AGH and YYL) and an Indiana Collaborative Research (IUCRG) grant (to AGH, AH and YYL).

Nonstandard abbreviations

NMDAR	N-methyl-D-aspartate receptor
nNOS	neuronal nitric oxide synthase
PSD95	postsynaptic density 95
CFA	complete Freund’s adjuvant

References

Abbadie C, Taylor BK, Peterson MA, Basbaum AI. Differential contribution of the two phases of the formalin test to the pattern of c-fos expression in the rat spinal cord: studies with remifentanil and lidocaine. Pain. 1997; 69:101–110. [PubMed: 9060019]

Al-Amin HA, Saade NE, Khani M, Atweh S, Jaber M. Effects of chronic dizocilpine on acute pain and on mRNA expression of neuropeptides and the dopamine and glutamate receptors. Brain research. 2003; 981:99–107. [PubMed: 12885430]

Amador TA, Verotta L, Nunes DS, Elisabetsky E. Involvement of NMDA receptors in the analgesic properties of psychotridine. Phytomedicine : international journal of phytotherapy and phytopharmacology. 2001; 8:202–206. [PubMed: 11417913]

Ashpole NM, Hudmon A. Excitotoxic neuroprotection and vulnerability with CaMKII inhibition. Molecular and cellular neurosciences. 2011; 46:720–730. [PubMed: 21316454]

Basbaum AI, Bautista DM, Scherrer G, Julius D. Cellular and molecular mechanisms of pain. Cell. 2009; 139:267–284. [PubMed: 19837031]

Berrino L, Oliva P, Massimo F, Aurilio C, Maione S, Grella A, Rossi F. Antinociceptive effect in mice of intraperitoneal N-methyl-D-aspartate receptor antagonists in the formalin test. European journal of pain. 2003; 7:131–137. [PubMed: 12600794]

Calvo M, Bennett DL. The mechanisms of microgliosis and pain following peripheral nerve injury. Experimental neurology. 2012; 234:271–282. [PubMed: 21893056]

Chen Y, Boettger MK, Reif A, Schmitt A, Uceyler N, Sommer C. Nitric oxide synthase modulates CFA-induced thermal hyperalgesia through cytokine regulation in mice. Molecular pain. 2010; 6:13. [PubMed: 20193086]

Chen Y, Stevens B, Chang J, Milbrandt J, Barres BA, Hell JW. NS21: re-defined and modified supplement B27 for neuronal cultures. Journal of neuroscience methods. 2008; 171:239–247. [PubMed: 18471889]

Christopherson KS, Hillier BJ, Lim WA, Bredt DS. PSD-95 assembles a ternary complex with the N-methyl-D-aspartic acid receptor and a bivalent neuronal NO synthase PDZ domain. The Journal of biological chemistry. 1999; 274:27467–27473. [PubMed: 10488080]

Chu YC, Guan Y, Skinner J, Raja SN, Johns RA, Tao YX. Effect of genetic knockout or pharmacologic inhibition of neuronal nitric oxide synthase on complete Freund's adjuvantinduced persistent pain. Pain. 2005; 119:113–123. [PubMed: 16297560]

Courtney MJ, Li LL, Lai YY. Mechanisms of NOS1AP action on NMDA receptornNOS signaling. Frontiers in cellular neuroscience. 2014; 8:252. [PubMed: 25221472]

D'Mello R, Marchand F, Pezet S, McMahon SB, Dickenson AH. Perturbing PSD-95 interactions with NR2B–subtype receptors attenuates spinal nociceptive plasticity and neuropathic pain. Molecular therapy : the journal of the American Society of Gene Therapy. 2011; 19:1780–1792. [PubMed: 21427709]

Deng L, Guindon J, Cornett BL, Makriyannis A, Mackie K, Hohmann AG. Chronic cannabinoid receptor 2 activation reverses paclitaxel neuropathy without tolerance or cannabinoid receptor 1-dependent withdrawal. Biological psychiatry. 2015; 77:475–487. [PubMed: 24853387]

Doucet MV, Levine H, Dev KK, Harkin A. Small-molecule inhibitors at the PSD-95/nNOS interface have antidepressant-like properties in mice. Neuropsychopharmacology : official publication of the American College of Neuropsychopharmacology. 2013; 38:1575–1584. [PubMed: 23446451]

Florio SK, Loh C, Huang SM, Iwamaye AE, Kitto KF, Fowler KW, Treiberg JA, Hayflick JS, Walker JM, Fairbanks CA, et al. Disruption of nNOS-PSD95 protein-protein interaction inhibits acute thermal hyperalgesia and chronic mechanical allodynia in rodents. British journal of pharmacology. 2009; 158:494–506. [PubMed: 19732061]

Garcia RA, Vasudevan K, Buonanno A. The neuregulin receptor ErbB-4 interacts with PDZ-containing proteins at neuronal synapses. Proceedings of the National Academy of Sciences of the United States of America. 2000; 97:3596–3601. [PubMed: 10725395]

Guindon J, Lai Y, Takacs SM, Bradshaw HB, Hohmann AG. Alterations in endocannabinoid tone following chemotherapy-induced peripheral neuropathy: effects of endocannabinoid deactivation inhibitors targeting fatty-acid amide hydrolase and monoacylglycerol lipase in comparison to reference analgesics following cisplatin treatment. Pharmacological research : the official journal of the Italian Pharmacological Society. 2013; 67:94–109. [PubMed: 23127915]

Harris BZ, Hillier BJ, Lim WA. Energetic determinants of internal motif recognition by PDZ domains. Biochemistry. 2001; 40:5921–5930. [PubMed: 11352727]

Huang YZ, Won S, Ali DW, Wang Q, Tanowitz M, Du QS, Pelkey KA, Yang DJ, Xiong WC, Salter MW, et al. Regulation of neuregulin signaling by PSD-95 interacting with ErbB4 at CNS synapses. Neuron. 2000; 26:443–455. [PubMed: 10839362]

Hudmon A, Lebel E, Roy H, Sik A, Schulman H, Waxham MN, De Koninck P. A mechanism for Ca2+/calmodulin-dependent protein kinase II clustering at synaptic and nonsynaptic sites based on self-association. The Journal of neuroscience : the official journal of the Society for Neuroscience. 2005; 25:6971–6983. [PubMed: 16049173]

Jaggi AS, Jain V, Singh N. Animal models of neuropathic pain. Fundamental & clinical pharmacology. 2011; 25:1–28. [PubMed: 20030738]

Kaneko M, Hammond DL. Role of spinal gamma-aminobutyric acidA receptors in formalin-induced nociception in the rat. The Journal of pharmacology and experimental therapeutics. 1997; 282:928–938. [PubMed: 9262360]

Latremoliere A, Woolf CJ. Central sensitization: a generator of pain hypersensitivity by central neural plasticity. The journal of pain : official journal of the American Pain Society. 2009; 10:895–926. [PubMed: 19712899]

Li LL, Ginet V, Liu X, Vergun O, Tuittila M, Mathieu M, Bonny C, Puyal J, Truttmann AC, Courtney MJ. The nNOS-p38MAPK pathway is mediated by NOS1AP during neuronal death. The Journal of neuroscience : the official journal of the Society for Neuroscience. 2013; 33:8185–8201. [PubMed: 23658158]

Luo CX, Zhu DY. Research progress on neurobiology of neuronal nitric oxide synthase. Neuroscience bulletin. 2011; 27:23–35. [PubMed: 21270901]

Malmberg AB, Yaksh TL. Antinociceptive actions of spinal nonsteroidal anti-inflammatory agents on the formalin test in the rat. The Journal of pharmacology and experimental therapeutics. 1992; 263:136–146. [PubMed: 1403779]

Miclescu A, Gordh T. Nitric oxide and pain: 'Something old, something new'. Acta anaesthesiologica Scandinavica. 2009; 53:1107–1120. [PubMed: 19702699]

Rameau GA, Chiu LY, Ziff EB. Bidirectional regulation of neuronal nitric-oxide synthase phosphorylation at serine 847 by the N-methyl-D-aspartate receptor. The Journal of biological chemistry. 2004; 279:14307–14314. [PubMed: 14722119]

Sattler R, Xiong Z, Lu WY, Hafner M, MacDonald JF, Tymianski M. Specific coupling of NMDA receptor activation to nitric oxide neurotoxicity by PSD-95 protein. Science. 1999; 284:1845–1848. [PubMed: 10364559]

Schmidt AP, Tort AB, Silveira PP, Bohmer AE, Hansel G, Knorr L, Schallenberger C, Dalmaz C, Elisabetsky E, Crestana RH, et al. The NMDA antagonist MK-801 induces hyperalgesia and increases CSF excitatory amino acids in rats: reversal by guanosine. Pharmacology, biochemistry, and behavior. 2009; 91:549–553.

South SM, Kohno T, Kaspar BK, Hegarty D, Vissel B, Drake CT, Ohata M, Jenab S, Sailer AW, Malkmus S, et al. A conditional deletion of the NR1 subunit of the NMDA receptor in adult spinal cord dorsal horn reduces NMDA currents and injury-induced pain. The Journal of neuroscience : the official journal of the Society for Neuroscience. 2003; 23:5031–5040. [PubMed: 12832526]

Steglitz J, Buscemi J, Ferguson MJ. The future of pain research, education, and treatment: a summary of the IOM report "Relieving pain in America: a blueprint for transforming prevention, care, education, and research". Translational behavioral medicine. 2012; 2:6–8. [PubMed: 24073092]

Tjolsen A, Berge OG, Hunskaar S, Rosland JH, Hole K. The formalin test: an evaluation of the method. Pain. 1992; 51:5–17. [PubMed: 1454405]

Tochio H, Mok YK, Zhang Q, Kan HM, Bredt DS, Zhang M. Formation of nNOS/PSD-95 PDZ dimer requires a preformed beta-finger structure from the nNOS PDZ domain. Journal of molecular biology. 2000; 303:359–370. [PubMed: 11031113]

Toro C, Deakin JF. NMDA receptor subunit NRI and postsynaptic protein PSD-95 in hippocampus and orbitofrontal cortex in schizophrenia and mood disorder. Schizophrenia research. 2005; 80:323–330. [PubMed: 16140506]

Ward SJ, Ramirez MD, Neelakantan H, Walker EA. Cannabidiol prevents the development of cold and mechanical allodynia in paclitaxel-treated female C57Bl6 mice. Anesthesia and analgesia. 2011; 113:947–950. [PubMed: 21737705]

Windebank AJ, Grisold W. Chemotherapy-induced neuropathy. Journal of the peripheral nervous system : JPNS. 2008; 13:27–46. [PubMed: 18346229]

Woolf CJ. Evidence for a central component of post-injury pain hypersensitivity. Nature. 1983; 306:686–688. [PubMed: 6656869]

Zhang H, Yoon SY, Zhang H, Dougherty PM. Evidence that spinal astrocytes but not microglia contribute to the pathogenesis of Paclitaxel-induced painful neuropathy. The journal of pain : official journal of the American Pain Society. 2012; 13:293–303. [PubMed: 22285612]

Zheng FY, Xiao WH, Bennett GJ. The response of spinal microglia to chemotherapyevoked painful peripheral neuropathies is distinct from that evoked by traumatic nerve injuries. Neuroscience. 2011; 176:447–454. [PubMed: 21195745]

Zhou HY, Chen SR, Pan HL. Targeting N-methyl-D-aspartate receptors for treatment of neuropathic pain. Expert review of clinical pharmacology. 2011; 4:379–388. [PubMed: 21686074]

Zhou L, Li F, Xu HB, Luo CX, Wu HY, Zhu MM, Lu W, Ji X, Zhou QG, Zhu DY. Treatment of cerebral ischemia by disrupting ischemia-induced interaction of nNOS with PSD-95. Nature medicine. 2010; 16:1439–1443.

Highlights

- IC87201 and ZL006 directly disrupt binding between PSD95 and nNOS *in vitro*.
- IC87201 and ZL006 protect against glutamate/glycine-induced neuronal cell death.
- Systemic IC87201 and ZL006 attenuate inflammatory and neuropathic pain behaviors.
- Unlike the NMDAR antagonist MK-801, IC87201 and ZL006 do not produce motor ataxia.
- The PSD95-nNOS protein-protein interface is a promising target for pain treatment.

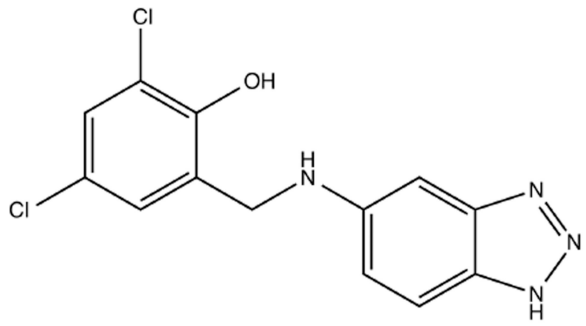

IC87201

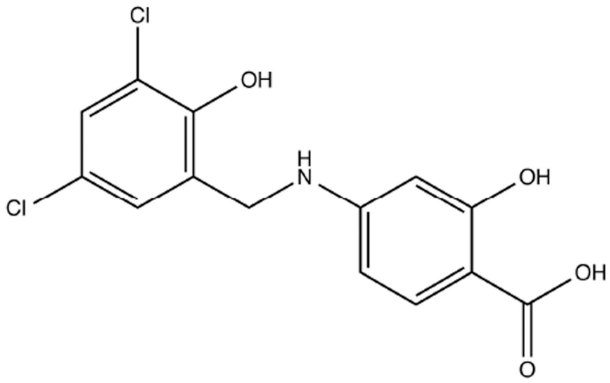

ZL006

Figure 1.
Chemical structures of small molecule PSD95-nNOS inhibitors IC87201 and ZL006.

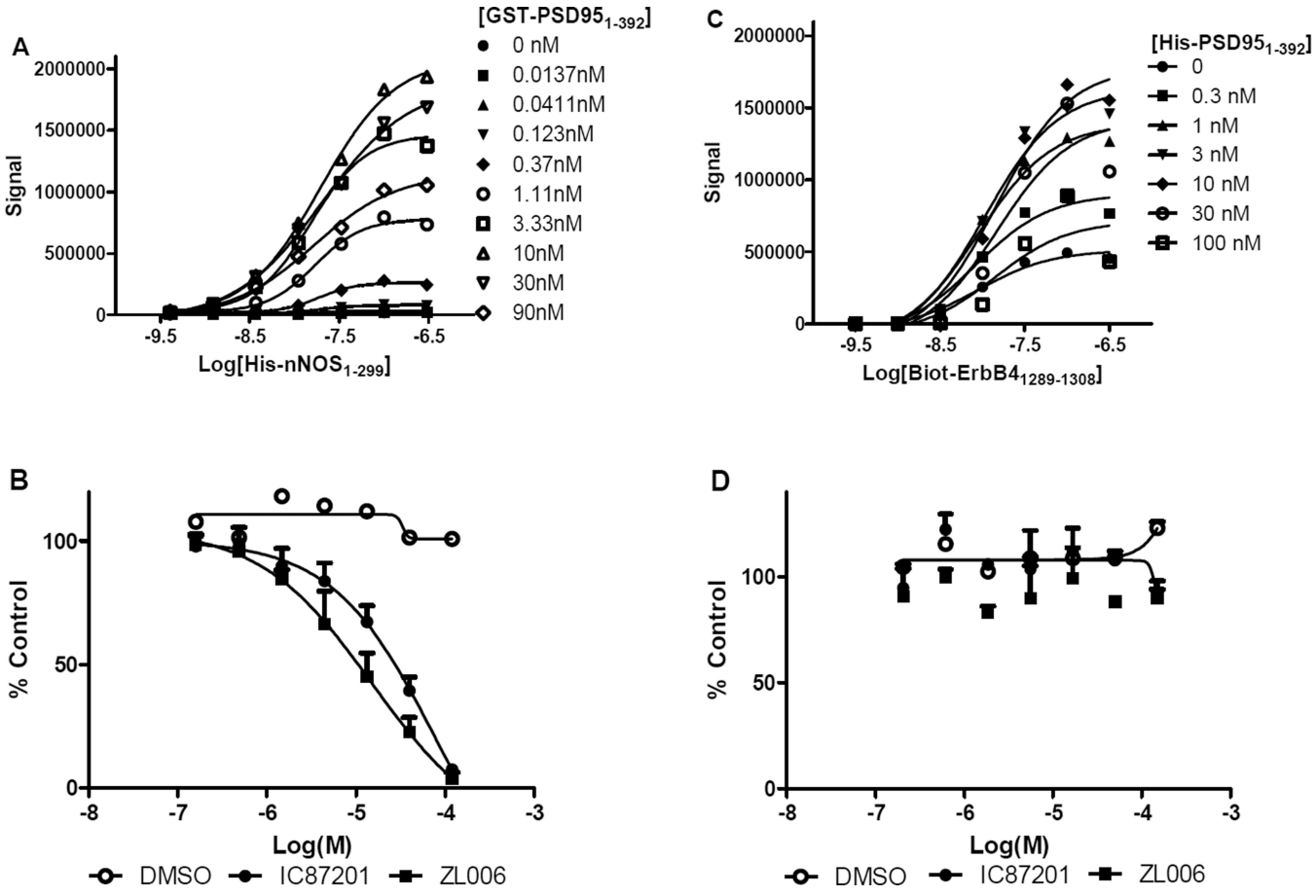

Figure 2.

Specificity of IC87201 and ZL006 for disrupting PSD95-nNOS binding demonstrated in AlphaScreen. **A**. Titration of GST-PSD95$_{1–392}$ and His-nNOS$_{1–299}$ from 0–175 nM. The EC_{50} determined is at 30 nM (n = 2). **B**. GST-PSD95$_{1–392}$ and His-nNOS$_{1–299}$ interactions were disrupted by IC87201 and ZL006 with an EC_{50} of 23.94 μM (n = 7) and 12.88 μM (n = 7) for IC87201 and ZL006, respectively. **C**. Titration of His-PSD95$_{1–392}$ and Biot-ErbB4$_{1289–1309}$ from 0–175 nM. The EC_{50} determined is at 10 nM (n = 2). **D**. IC87201 and ZL006 did not disrupt Biot-ErbB4$_{1289–1308}$ and His-PSD95$_{1–392}$ protein-protein interactions.

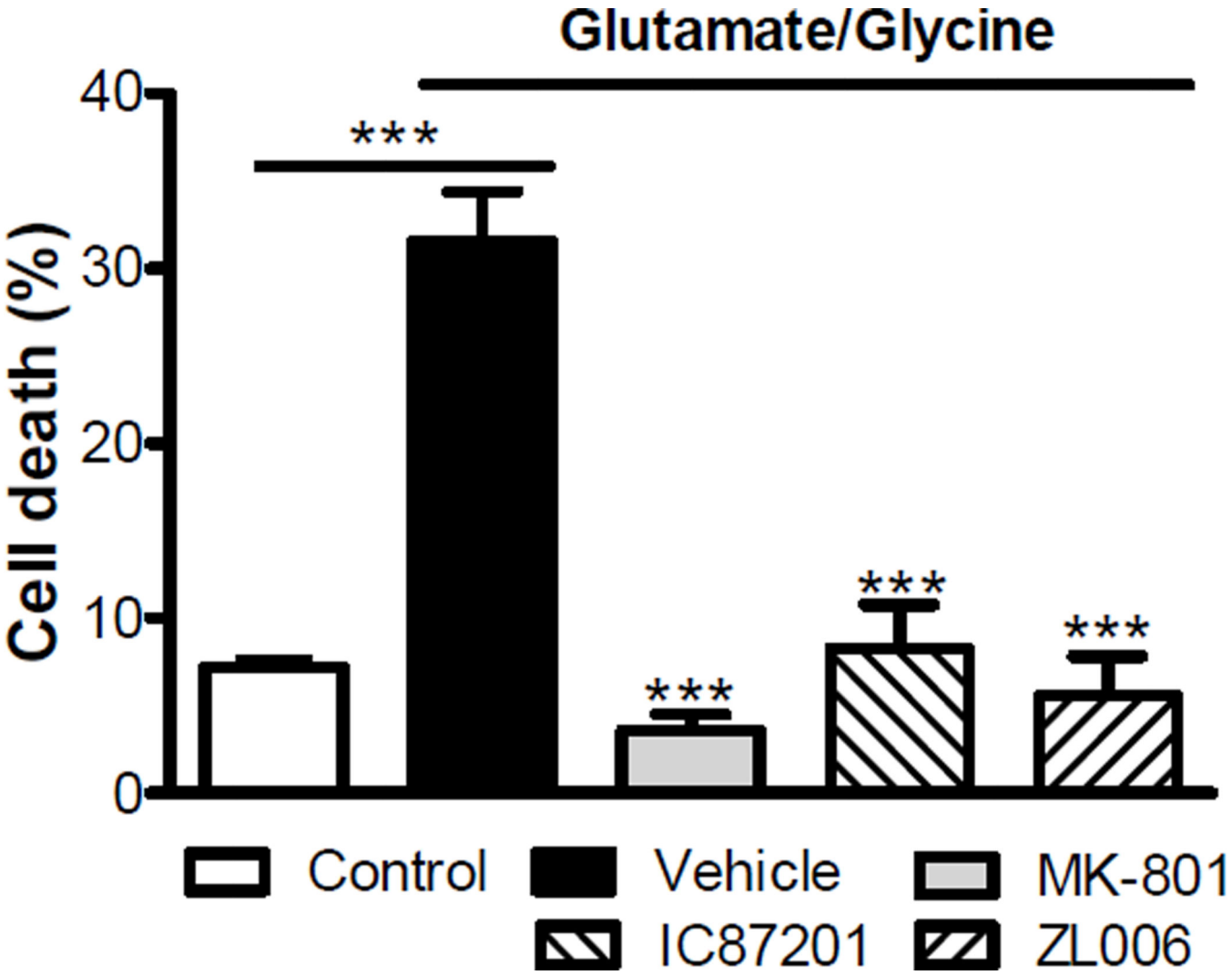

Figure 3.

Effects of small molecule inhibitors on cortical neuronal cell death induced by glutamate. Pretreatment of small molecule inhibitors, IC87201 (10 μM) and ZL006 (10 μM) protected against glutamate treatment induced cell death in cortical neuronal cells with efficacy similar to MK-801 (20 μM). **p < 0.01; ***p < 0.001 (one-way ANOVA).

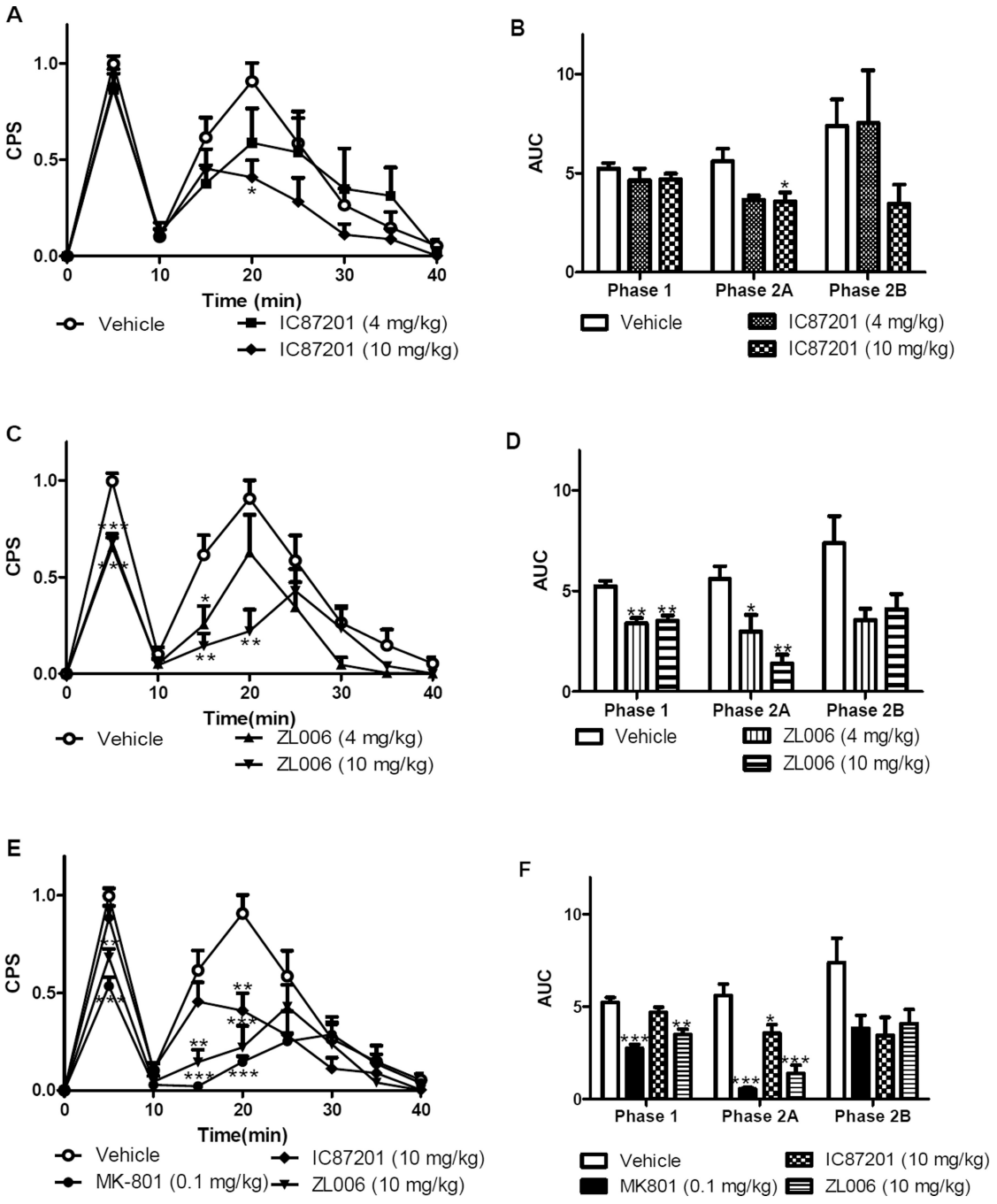

Figure 4.

Effects of small molecule PSD95-nNOS inhibitors on formalin-induced pain behaviors. **A, B** IC87201 (4 and 10 mg/kg i.p.) suppresses formalin-induced nociceptive behaviors during phase 2A (n = 6–8). **C, D** ZL006 (4 and 10 mg/kg i.p.) suppresses formalin-induced nociceptive behaviors during phase 1 and phase 2A but not during phase 2B (n = 6–8). **E, F** Comparison of maximally efficacious doses of small molecule inhibitors with NMDAR antagonist MK-801 (0.1 mg/kg i.p.) (n = 6–8). *p < 0.05; **p < 0.01; ***p < 0.001 versus control.

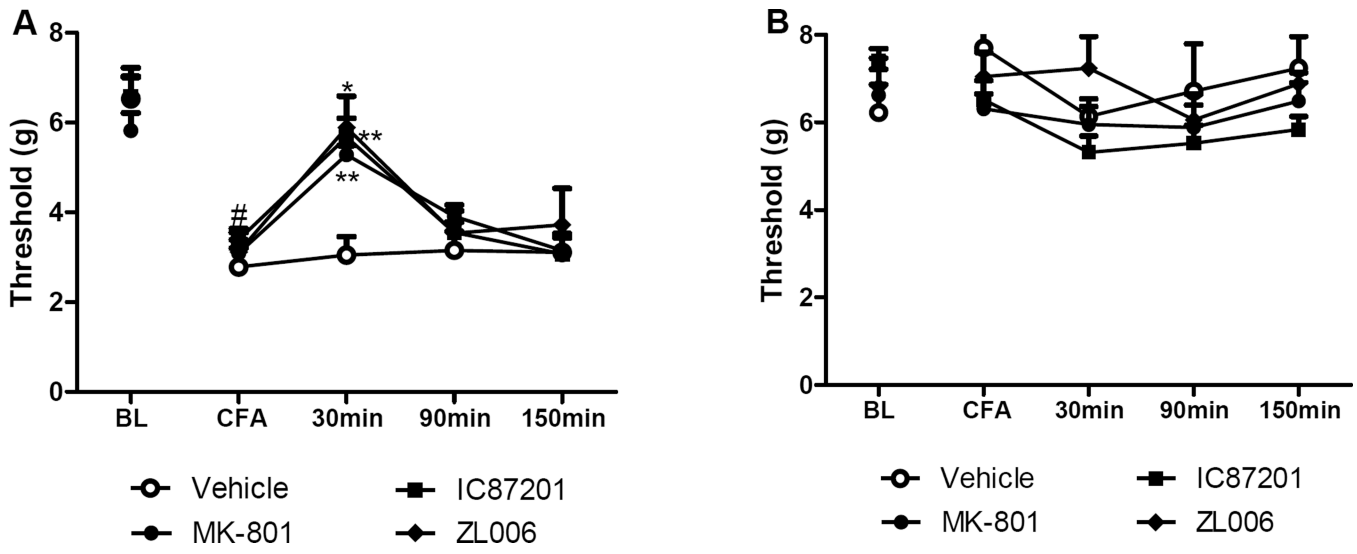

Figure 5.

Effects of small molecule inhibitors on CFA induced mechanical allodynia. **A**. IC87201 (10 mg/kg, ip) and ZL006 (10 mg/kg, ip) suppressed CFA-induced mechanical allodynia similar to MK-801 (0.1 mg/kg i.p.). **B**. IC87201 and ZL006 administration did not alter mechanical thresholds in the contralateral paw. (n = 6 per group). *p < 0.05; **p <0.01; ***p <0.001. # p < 0.01 difference between baseline (BL) and post CFA pre-injection response.

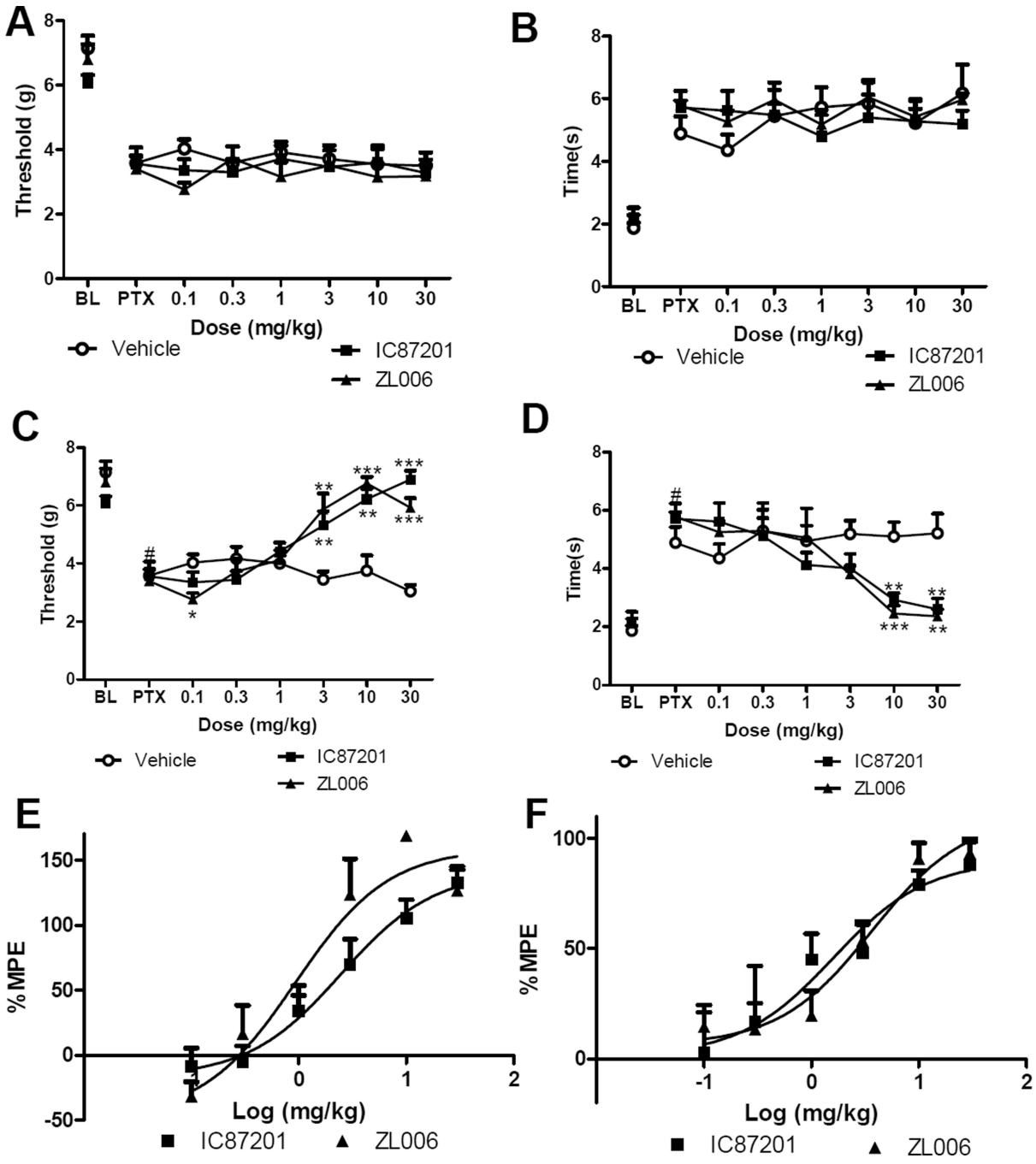

Figure 6.

Dose response of small molecule inhibitors on paclitaxel-induced mechanical and cold allodynia. **A, B**. Pre-drug mechanical paw withdrawal thresholds (**A**) and cold response latencies (**B**) during the maintenance phase of paclitaxel-induced allodynia. Data are plotted relative to pre-paclitaxel baseline responding. **C, D**. Dose response of IC87201 and ZL006 in suppressing paclitaxel-induced (**C**) mechanical and (**D**) cold responsiveness. **E, F**. % Maximal possible effect (%MPE) of IC87201 and ZL006 in suppressing (**E**) mechanical and (**F**) cold allodynia used for ED_{50} calculation (n = 6 per group).*p < 0.05; **p < 0.01; ***p <

0.001 versus vehicle. # $p < 0.01$ difference between baseline (BL) and post pacltiaxel (PTX) pre-injection response.

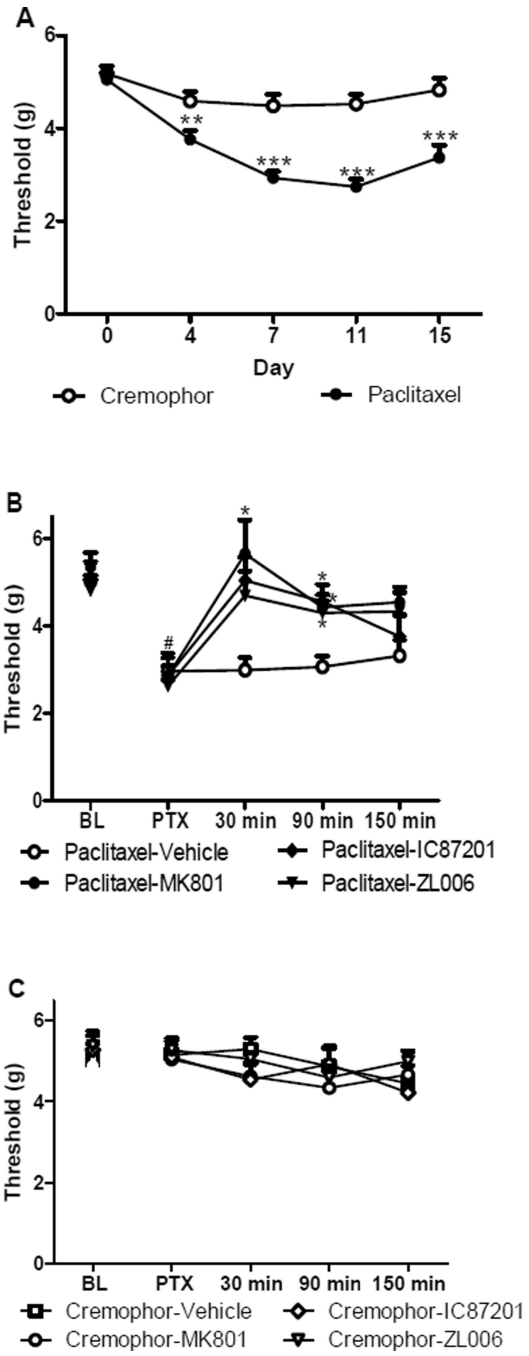

Figure 7.

Small molecule PSD95-nNOS inhibitors suppress paclitaxel-induced mechanical allodynia. **A**. Paclitaxel but not cremophor vehicle treatment induced mechanical allodynia. **B**. IC87201 (10 mg/kg, i.p) and ZL006 (10 mg/kg, i.p.) attenuate paclitaxel-induced mechanical allodynia, similar to MK-801 (0.1 mg/kg i.p.). **C**. IC87201, ZL006 and MK801 treatment did not alter mechanical paw withdrawal thresholds in the absence of paclitaxel treatment. (n = 6 per group). *p < 0.05; **p < 0.01; ***p < 0.001 versus vehicle. #p < 0.01 difference between baseline (BL) and post paclitaxel (PTX) pre-injection threshold.

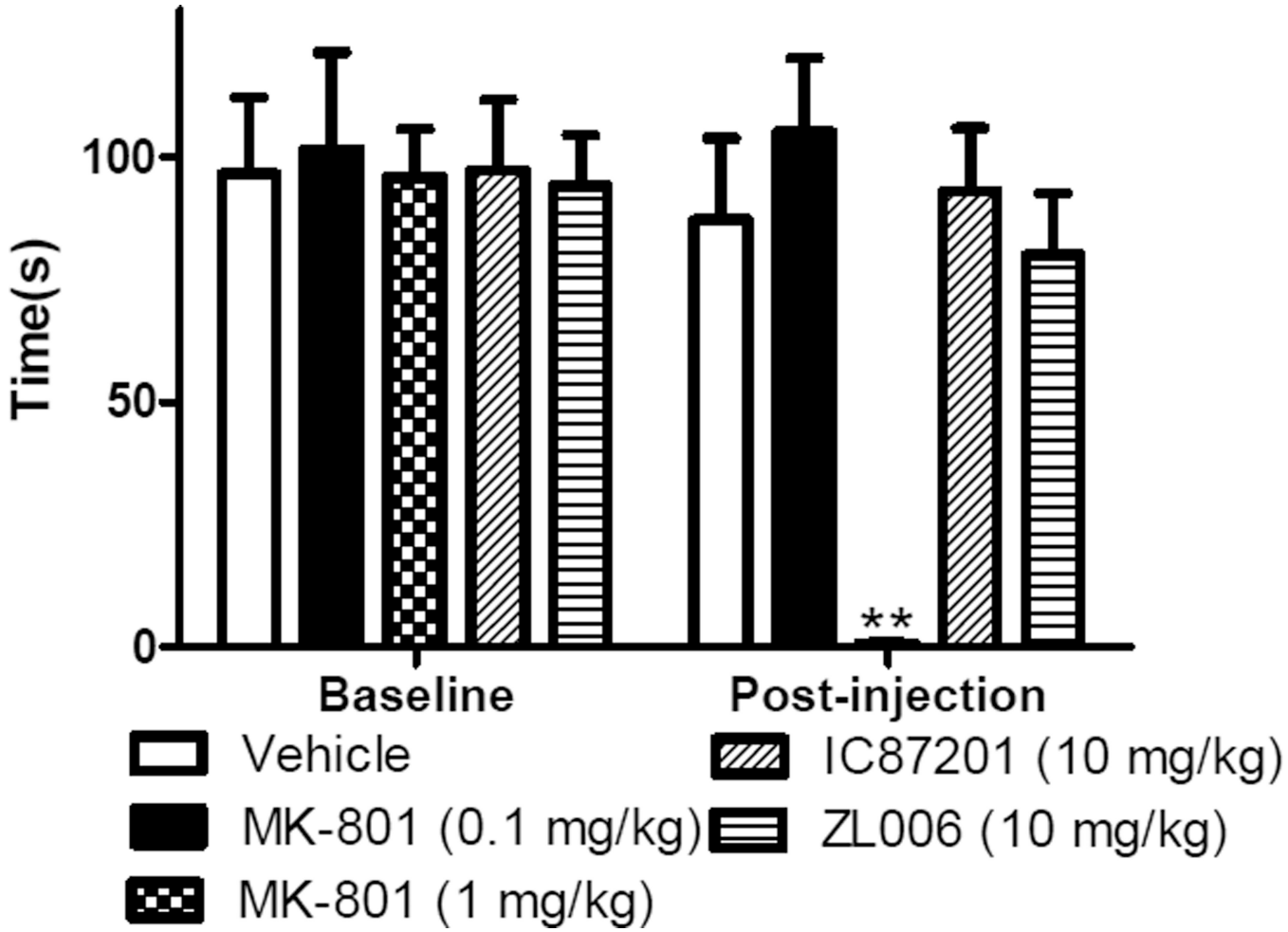

Figure 8.

PSD95-nNOS inhibitors IC87201 and ZL006 (10 mg/kg i.p.) did not produce motor ataxia in the rota rod test. A high (1 mg/k i.p.) but not a low (0.1 mg/kg i.p.) dose of MK-801 decreased latency to fall off a rotating drum in the rota-rod test. (n= 6–11 per group). **p < 0.01 versus vehicle.

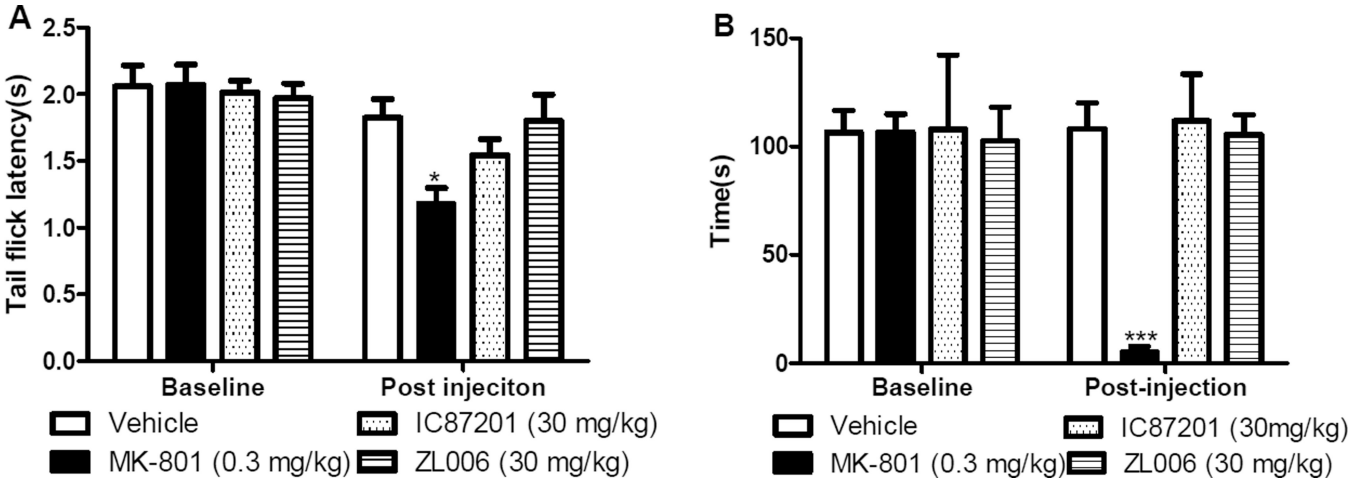

Figure 9.

Small molecule PSD95-nNOS inhibitors at supramaximal doses (30 mg/kg i.p.) did not produce tail flick antinociception/hyperalgesia or produce motor ataxia. **A**. IC87201 and ZL006 did not alter tail flick latencies whereas MK-801 (0.3 mg/kg i.p.) produced hyperalgesia in the same test. **B**. In the same animals, small molecule PSD95-nNOS inhibitors (30 mg/kg i.p.) did not impair motor coordination whereas MK-801 (0.3 mg/kg i.p.) produced robust motor ataxia. (n= 6 per group).*$p < 0.05$;***$p < 0.001$.